

# FEA Information Inc. Global News & Technical Information

Dedicated to the Global Engineering Community



LEAP

ALTAIR-Italy

DYNAMAX

ANSYS-China

DYNALIS

GISSETA

DYNAmore

FLOTREND

KOSTECH

ERAB

THEME

MFAC

CAD-FEM

Prof Genarro Monacelli

Dr. David Benson

Dr. Alexey I. Borovkov

Dr. Ted Belytschko

Dr. Taylan Altan

Dr. Bhavin V. Mehta

Prof. Ala Tabiei



**FEA Information Inc.**

**Global News  
&  
Industry Information**

**Volume 2**

**Issue 6-2002**

**June**

Editor: Trent Eggleston  
Technical Writer Arthur B. Shapiro  
Technical Writer David Benson  
Graphic Designer Wayne Mindle  
Feature Director Marsha Victory

**Purpose:**

The purpose of our publication is to provide technical and industry information

**In This Issue:**

03	One Model – One Code - LSTC
05	June Publication Showcase
17	Getting Started with LS-DYNA Chapter 4
24	FEA Web Site Summary & Events
25	Visteon – EnSight – MSC.Nastran – LS-DYNA
27	Participant Listing
28	FIRST ANNOUNCEMENT AND CALL FOR PAPERS - 4th European LS-DYNA Conference

**The contents of this publication is deemed to be accurate and complete. However, FEA Information Inc. doesn't guarantee or warrant accuracy or completeness of the material contained herein. All trademarks are the property of their respective owners. This publication is published for FEA Information Inc., Copyright 2002. All rights reserved. Not to be reproduced in hardcopy or electronic format**

## **One Model – One Code © Livermore Software Technology, 2002 Perspective on LS-DYNA in the Future**

As computer power grows exponentially, and competitive pressures and liability issues increase, engineers are expected to perform more detailed analyses of their product designs than ever before. In addition, the analyses are becoming increasingly multi-disciplinary. For example, twenty years ago, automobile handling studies were performed with rigid body dynamics codes, and tires were analyzed separately with quasi-static finite element models. Today, vehicle dynamics are modeled in LS-DYNA with a combination of rigid bodies and deformable elements, including detailed finite element models of the tire. The tire models not only include the lay-up of the belts, but also the effect of the tire deformation on the tire pressure. Coupled Lagrangian-Eulerian calculations by LS-DYNA of hydroplaning tires compare well with experiments. In the near future we anticipate handling studies of hydroplaning vehicles that combine the current handling models with the hydroplaning tire models.

### **Current practices:**

The current practice in industry is to prepare separate models for each type of analysis, with each type of analysis being handled by a separate application code. This practice, which has been motivated in the past by both software and hardware limitations, is wasteful of engineering time. The models are incompatible and stored in separate input files, each with their own format. Every time a design change is made, all the models must be updated. This inevitably introduces errors and delays. Multi-physics problems are usually impractical due to the incompatible models. Even if the results of one analysis can be used as input in another, the effects of the different physics are propagated only in one direction.

The personnel costs are high with the current practice. The careers paths of engineers are determined by which codes they know how to use. Analysts have to spend the time to learn each of the different codes for the analyses they perform. Bottlenecks in engineering analysis can occur when a department has only a few people skilled in one code and there is a sudden demand for its analyses.

### **Future:**

In the future, there will be one model for all applications. Analysts will work in parallel to reduce the time to produce the initial model. In crash, one model for frontal, side, offset, and rear impacts is just becoming a reality. Mesh adaptivity will be used to adjust the mesh density based on the crash location. Durability, NVH, and crash models will be identical, which means that only one model will be revised for design changes and checked for errors. Multi-physics problems will be addressed easily. Database management will be much easier with only one model definition to track.

### **One Code:**

The current practice is to use specialized codes for each problem. Multi-physics problems are difficult, if not impossible, to solve in this manner. Analysts must be trained in the use of each specialized code, and if multi-physics problems are to be handled, a manager must find an analyst skilled in using the appropriate combination of codes, or assemble a team with the required skills regardless of the size or priority of the problem.

In the future, industry will use one code with a broad range of physics and algorithms. Coupled solutions of multi-physics problems will be the norm instead of the exception. Fluid-structure interaction problems, such as tire hydroplaning and airbag deployment, will be solved in a fully coupled manner. Thermo-mechanical problems, e.g., hot forging, are common and will be solved

appropriately. Multi-disciplinary optimization will be routine once multi-physics analysis is accepted as the industry standard.

An analyst can work on related problems without learning new software. Analyst productivity will greatly increase since all the analyses will be performed with a single model. This introduces new flexibility in the analyst's career path and in the management of analysis groups.

### **Multi-Stage Modeling:**

Just as one model may be used in parallel for different types of analyses, one model will also be used in multi-stage problems that require sequential simulations. For example, in stamping, the analysis can consist of three stages:

1. Binderwrap (put flat blank on curved die-implicit dynamics).
2. Sheet metal stamping (explicit with mass scaling).
3. Spring back (dies removed-implicit static).

It's natural to want to use the results of a manufacturing analysis in a performance simulation. Extending the previous example to crash and beyond, we can add the following:

1. Sheet metal stamping of parts introduces texturing and thinning
2. Static initialization due to gravitational loading prior to performance cycle.
3. Performance analyses:
  - a. Crash simulation accounts for effects of manufacturing processing
  - b. NVH.
  - c. Fatigue predictions accounting for residual stresses and cycle history.

### **Multi-Formulations:**

No single solution method is suitable for all applications. Codes need to have multiple algorithms for the same physics. In solid mechanics, for example, different element formulations are necessary for nonlinear problems with large deformations and for linear problems, such as eigenvalue and linear structural analyses. In a similar manner, fluids problems require different flow solvers depending on if the fluid is compressible or incompressible, the flow is supersonic or acoustic. Depending on the time scale, implicit or explicit time integration methods may be more efficient.

### **Multi-Processing:**

Massively Parallel Processing (MPP) is here to stay. It is a necessary element for making large-scale, multi-disciplinary analyses a reality. MPP is no longer just for the national laboratories and NSF-supported computer centers. Desktop MPP is available under Unix, Windows, and the Linux environments on virtually any machine, ranging from high performance RISC architectures to the Pentium IV. The availability of high-speed networks means that the individual processors no longer need to be in the same room, allowing the processors in a department to be tied together at night for large MPP jobs. Computer centers now have MPP farms where many parallel jobs are running simultaneously on subsets of processors. Based on current benchmarks, 12 to 64 processors are preferred to LS-DYNA.

### **Conclusion:**

Market forces and government regulations are driving industry to perform more analyses than ever before. Fortunately, the computer hardware is improving rapidly, making not only more analyses possible, but also making routine, types of analyses that were not possible only a decade ago. To address the additional demands placed on analysts, one model being run on one code to produce many types of results is the development goal of LSTC for LS-DYNA.

**FEA Information Inc. June Showcased Presentation  
From the 7<sup>th</sup> International LS-DYNA Users Conference**

**A Material Model for Transversely Anisotropic Crushable Foams In LS-DYNA**

**MAT\_TRANSVERSELY\_ANISOTROPIC\_CRUSHABLE\_FOAM**

**Material Law 142**

**Andreas Hirth**

DaimlerChrysler

HPC X414

71059 Sindelfingen, Germany

Tel.: 07031-90-87781

Fax: 07031-90-87516

email: andreas.hirth@daimlerchrysler.com

**Paul Du Bois**

Consulting engineer

63071 Offenbach/ Main, Germany

**Dr. Klaus Weimar**

DYNAmore

70565 Stuttgart-Vaihingen, Germany

*Keywords:*

Crushable foam, energy absorption, material law, transversely anisotropic

## **ABSTRACT**

Recently new materials were introduced to enhance different aspects of automotive safety while minimizing the weight added to the vehicle. Such foams are no longer isotropic but typically show a preferred strong direction due to their manufacturing process. Different stress/ strain curves are obtained from material testing in different directions. A new material model was added to the LS-DYNA code in order to allow a correct numerical simulation of such materials. Ease-of-use was a primary concern in the development of this user-subroutine: we required stress/ strain curves from material testing to be directly usable as input parameters for the numerical model without conversion. The user-subroutine is implemented as MAT\_TRANSVERSELY\_ANISOTROPIC\_CRUSHABLE\_FOAM, Mat law 142 in LS-DYNA Version 960-1106. In this paper we summarize the background of the material law and illustrate some applications in the field of interior head-impact. The obvious advantage of incorporating such detail in the simulation lies in the numerical assessment of impacts that are slightly offset with respect to the foam's primary strength direction.

## **INTRODUCTION**

In this paper we will be studying a class of transversely anisotropic, crushable, low-density foams. Such materials are used in energy-absorbing structures to enhance automotive safety in low velocity (bumper impact, interior head impact) and medium high (pedestrian safety) velocity applications. The potential advantage lies in the high longitudinal strength of the material in comparison to isotropic foams with the same density.

The numerical simulation of such foams requires an anisotropic elastoplastic material law with a flow rule allowing for high permanent volumetric deformation. The anisotropic feature of the material model should thereby allow to properly represent the off-axis material response. In this report existing anisotropic material models for foams in the LS-DYNA code are investigated first. It is shown that they have certain deficiencies rendering them unsuitable to simulate the behavior of anisotropic crushable foams under off-axis loading conditions. Consequently a new material model was developed and added to LS-DYNA as a user-subroutine in order to overcome these problems.

## APPROACH

### Summary of Test Results

To quantify the mechanical behavior of anisotropic crushable foams, a testing matrix is proposed containing compression, tension and shear tests according to the following table in figure 1.

loading	Angle $\vartheta$ between load direction and extrusion direction
compression	0°, 5°, 10°, 15°, 25°, 30°, 35°, 45°, 60°, 90°
tension	0°, 90°
shear	0°, 90°

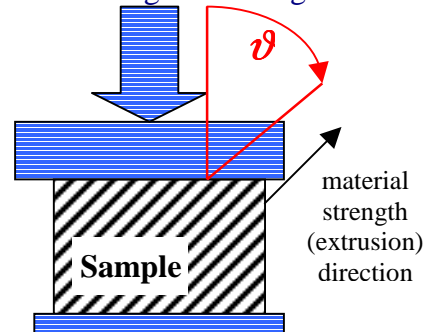


**Figure 1.** Testing matrix and sketch for the compression tests

The samples for offset loading were manufactured by a waterjet cutting technology. At least the compression tests should then be performed quasistatically and dynamically for a number of different strain rates. A typical material with a transversely anisotropic crushable behavior is *Strandfoam*<sup>1</sup>. For this material with a density of 2.5pcf the complete set of tests has been performed.

The rate dependency of these materials will not be treated further here since we want to emphasize the anisotropic aspect of the material behavior. Extension of our material law to include rate dependency is a trivial though extensive matter.

The main information that can be deduced from the test results is the variation of the foam's compressive strength as a function of the angle  $\vartheta$  between the loading direction and the longitudinal (extrusion- or strong) direction of the foam. The numerical reproduction of the stress/ strain characteristics for the material in different directions is the main issue of this investigation. An example of such a characteristic for *Strandfoam 2.5pcf* is drawn below.

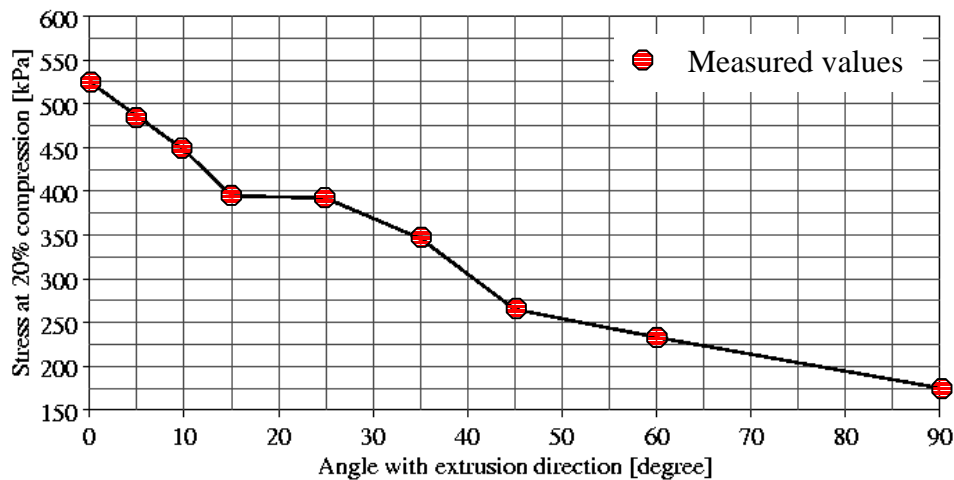


**Figure 2.** Off-axis strength for *Strandfoam 2.5pcf* at 20% compression

<sup>1</sup> Trademark of the Dow Chemical Company



Figure 2 shows the off-axis strength for *Strandfoam 2.5pcf* at 20% compression as taken from the test results (stress values for loading at a strain rate of 10/s). The compressive resistance of the material differs by a factor of 3 between the strong and weak directions and drops fast within the first 15° of oblique loading.

**Material law MAT\_HONEYCOMB (Mat 26)**

The only orthotropic, crushable material laws in LS-DYNA suitable for treatment of low density foams (zero Poisson effect) are MAT\_HONEYCOMB (Mat 26) and MAT\_MODIFIED\_HONEYCOMB (Mat 126). In the MAT\_HONEYCOMB, a material reference system is defined by the user. In the case of a transversely anisotropic foam, one of the axes of this system should coincide with the extrusion direction in the undeformed configuration. During the analysis, this material system follows the element rigid body rotation in every brick element. The material law is formulated by uncoupling of the stress tensor components in the material system: every component has a proper yield value independently of the other 5 stress components.

$$|\sigma_{ij}| \leq \sigma_{ij}^y(\epsilon_v) \tag{1}$$

The corresponding yield surface is a rectangular box in principal stress space. This can lead to a surprising behavior of the material model under offset loading. For instance, it is not possible to generate realistic input data for this material law that will lead to an isotropic behavior of the material.

As an example, consider uniaxial loading (in figure 3: compression) in the global x-direction. The material extrusion direction corresponds to the 1-axis of the material system:

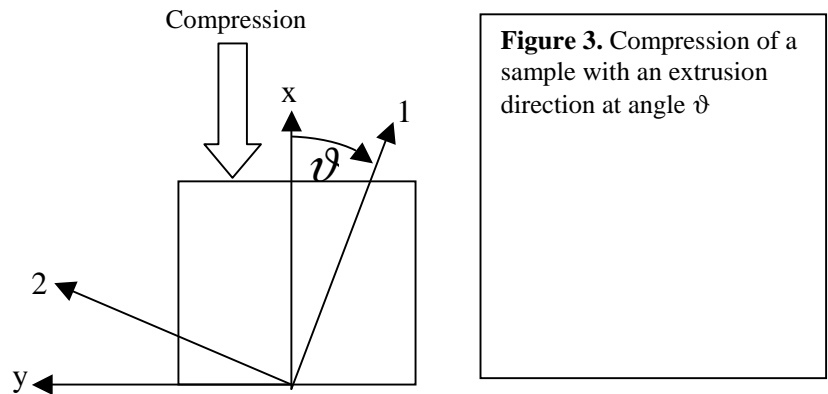


**Figure 3.** Compression of a sample with an extrusion direction at angle  $\vartheta$

If we ignore the third dimension then the stress transformation is:

$$\begin{pmatrix} \sigma_{xx} & 0 \\ 0 & 0 \end{pmatrix} = \begin{pmatrix} \cos\vartheta & \sin\vartheta \\ -\sin\vartheta & \cos\vartheta \end{pmatrix} \begin{pmatrix} -\sigma_{11}^y & -\sigma_{12}^y \\ -\sigma_{12}^y & -\sigma_{22}^y \end{pmatrix} \begin{pmatrix} \cos\vartheta & -\sin\vartheta \\ \sin\vartheta & \cos\vartheta \end{pmatrix} \tag{2}$$

If we assume the deformations to be large enough to cause plastification of all material stress components (other solutions are possible), then (in the case of compression) equation (2) leads to:

$$\begin{pmatrix} \sigma_{xx} & 0 \\ 0 & 0 \end{pmatrix} = \begin{pmatrix} \cos\vartheta & \sin\vartheta \\ -\sin\vartheta & \cos\vartheta \end{pmatrix} \begin{pmatrix} \sigma_{11}^y & \sigma_{12}^y \\ \sigma_{12}^y & \sigma_{22}^y \end{pmatrix} \begin{pmatrix} \cos\vartheta & -\sin\vartheta \\ \sin\vartheta & \cos\vartheta \end{pmatrix} \tag{3}$$



Since all material stress components will be negative and the yield stresses are necessarily positive. Solving equation (3) gives:

$$|\sigma_{xx}| = (\cos \vartheta)^2 \sigma_{11}^y + (\sin \vartheta)^2 \sigma_{22}^y + 2 \cos \vartheta \sin \vartheta \sigma_{12}^y \quad (4)$$

Clearly for known (measured) strong and weak directions in the material, the off-axis strength depends upon the shear strength. The results can be amazing, as for non-zero shear strength, the off-axis strength will exceed the material strength in the principal material axes directions.

Equation (4) was evaluated for angles between 0° and 90° for material data corresponding to *Strandfoam 2.5pcf* and drawn in figure 4 in comparison to the measured values. Off-axis strength is estimated from experimental values for compression at 20% strain, thus using:

$$\begin{aligned} \sigma_{11}^y &= 525 \text{ kPa} & (\vartheta = 0^\circ) \\ \sigma_{22}^y &= 175 \text{ kPa} & (\vartheta = 90^\circ) \\ \sigma_{12}^y &= 175 \text{ kPa} & (\text{shear}) \end{aligned} \quad (5)$$

The predicted overestimation of off-axis strength (figure 4, blue curve) is confirmed in LS-DYNA simulations of compression tests using MAT\_HONEYCOMB (Mat26).

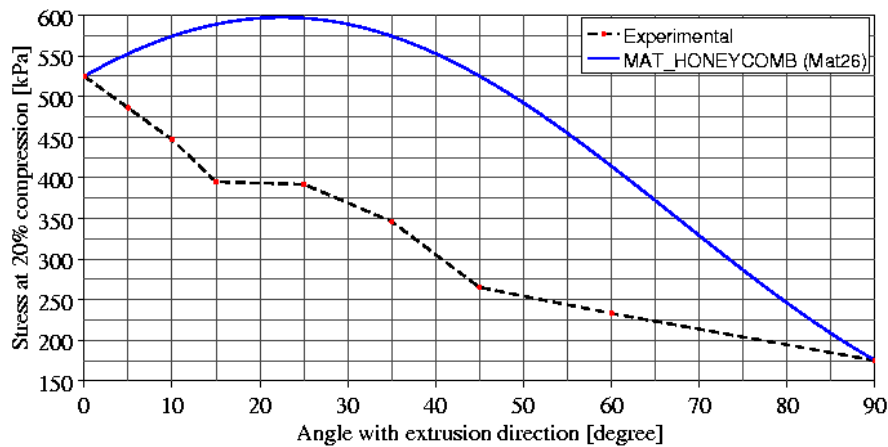


**Figure 4.** Off-axis strength for *Strandfoam 2.5pcf* at 20% compression, experimental values (black dashed line) and theoretical values with Mat26 (blue line)

***Material law MAT\_TRANSVERSELY\_ANISOTROPIC\_CRUSHABLE\_FOAM (Mat 142)***

A user subroutine MAT\_USER\_DEFINED was developed and added at first to LS-DYNA in order to correct the systematic overestimation of the off-axis strength by MAT\_HONEYCOMB (and MAT\_MODIFIED\_HONEYCOMB) for transversely orthotropic material and to allow an easier calibration of the numerical model to measurements. The addition of anisotropic user material laws in LS-DYNA was made possible in a standardized way (/1/).

The principal characteristics of the material law in question are the following:

- transversely anisotropic elasto-plastic model
- Tsay-Wu yield surface
- variable coefficients depending upon volumetric strain

- optional definition of a test curve for off-axis loading
- zero Poisson coefficient under longitudinal loads  
(flow surface is spherical in stress space)

A Tsay-Wu surface is a fixed, quadratic surface in 6-dimensional stress-space that is used traditionally as a failure surface for the numerical simulation of composite materials. The application here is quite different since we use the Tsay-Wu surface as a yield surface which is not fixed in stress space, but ‘hardens’ or ‘softens’ as a function of volumetric strain. The evolution of the yield surface is directional and emulates the evolution of the material yield stress along the different material axes. A further modification of the traditional Tsay-Wu approach lies in the symmetrisation of the yield surface: a single yield value for tension and compression is determined depending upon the current value of the volumetric strain as in equation (6).

$$\varepsilon_v = 1 - \frac{V}{V_0} \Rightarrow \sigma^{yc} = \sigma^{yt} = \sigma^y(\varepsilon_v) \quad (6)$$

Since our applications will mainly consist of a single loading cycle we feel this simplification is justifiable and adds considerably to the numerical robustness of the material model.

With these assumptions the transversely anisotropic Tsay-Wu yield surface is defined as:

$$\begin{aligned} & F_{11}\sigma_{xx}^2 + F_{22}\sigma_{yy}^2 + F_{22}\sigma_{zz}^2 + \\ & F_{44}\sigma_{xy}^2 + F_{55}\sigma_{yz}^2 + F_{44}\sigma_{zx}^2 + \\ & 2F_{12}\sigma_{xx}\sigma_{yy} + 2F_{23}\sigma_{zz}\sigma_{yy} + 2F_{12}\sigma_{xx}\sigma_{zz} \leq 1 \end{aligned} \quad (7)$$

Thus in equation (7) 6 coefficients have to be determined by matching the following load cases as a function of volumetric strain:

- longitudinal tension and compression ( $F_{11}$ )
- transversal tension and compression ( $F_{22}$ )
- strong shear ( $F_{44}$ )
- weak shear ( $F_{55}$ )
- off-axis tension and compression strong/weak ( $F_{12}$ )
- off-axis tension and compression weak/weak ( $F_{23}$ )

The coefficients of the yield surface are determined for every value of the current volumetric strain from the corresponding yield values of the stress in each material direction.

$$F_{11} = \frac{1}{\sigma_{xx}^y \sigma_{xx}^y} \quad (8)$$

Under longitudinal compression we obtain equation (8).

For the transversal directions we obtain equation (9).

$$F_{22} = \frac{1}{\sigma_{yy}^y \sigma_{yy}^y} \quad (9)$$

Similarly the pure shear condition yields to equation (10) and equation (11).

$$F_{44} = \frac{1}{\sigma_{xy}^y \sigma_{xy}^y} = \frac{1}{\sigma_{zx}^y \sigma_{zx}^y} \quad (10)$$

$$F_{55} = \frac{1}{\sigma_{yz}^y \sigma_{yz}^y} \quad (11)$$

In the classical Tsay-Wu surface, the remaining coefficients are calculated as in equations (12) and (13).

$$F_{12} = \frac{-1}{2} \sqrt{F_{11} F_{22}} \quad (12)$$

$$F_{23} = \frac{-1}{2} F_{22} \quad (13)$$

In our approach it was decided to fit a curve for off-axis loading under theta degrees between longitudinal (=x) and transversal (=y or z) directions in order to determine a reasonable value for  $F_{12}$  as a function of volumetric strain, where  $\sigma_{\vartheta\vartheta}$  is the stress, measured in the off-axis loading experiment.

Solving the yield condition under off-axis loading for  $F_{12}$  gives equation (14).

$$F_{12} = \frac{1}{2 \cos^2 \vartheta \sin^2 \vartheta \sigma_{\vartheta\vartheta}^2} - \frac{F_{11} \cos^2 \vartheta}{2 \sin^2 \vartheta} - \frac{F_{22} \sin^2 \vartheta}{2 \cos^2 \vartheta} - \frac{F_{44}}{2} \quad (14)$$

Once all the coefficients of the Tsay-Wu yield function have been determined, it is possible to estimate the off-axis strength of the foam (as we did for material law 26 in figure 4). Again we use the measurements of *Strandfoam 2.5pcf* (see equation (5)) to evaluate an example numerically.

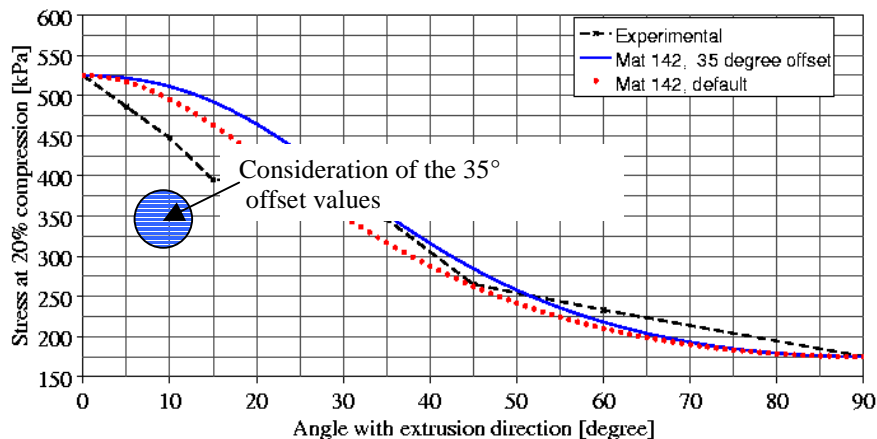


**Figure 5.** Off-axis strength for *Strandfoam 2.5pcf* at 20% compression, experimental values (black dashed line) and theoretical values with Mat 142 (blue line with 35° offset, red dotted line default)

In figure 5 we have compared the values obtained from the default Tsay-Wu model (equation (12), red dotted line) with our modified model where the test curve for loading under 35° was used (equation (14), blue line). In this case it seems, that the default Tsay-Wu gives better overall results than the consideration of the 35° offset values.

### **Validation for Material law *MAT\_TRANSVERSELY\_ANISOTROPIC\_CRUSHABLE\_FOAM (Mat 142)***

A numerical model for *Strandfoam 2.5pcf* was created under the following assumptions :

- Shear stress was compared to transverse stress to show that yield in shear and transverse direction are similar for small strain values, a similar dependency of volumetric strain for shear is assumed in the model as in the transverse direction (i.e. we use the same curve).
- The transition from a plateau-type stress-strain curve to a stress-strain curve with non-zero gradient and generally lower stress values, takes place around 35° offset, therefore the stress-strain curve for loading under 35° was used to construct the yield surface and determine  $F_{12}$ .

Simulations of dynamic compression tests were then performed on a simple model for all tested loading angles at a strain rate of 100/s. The offset loading causes shear deformation as shown in the example in figure 6 (35° offset loading).

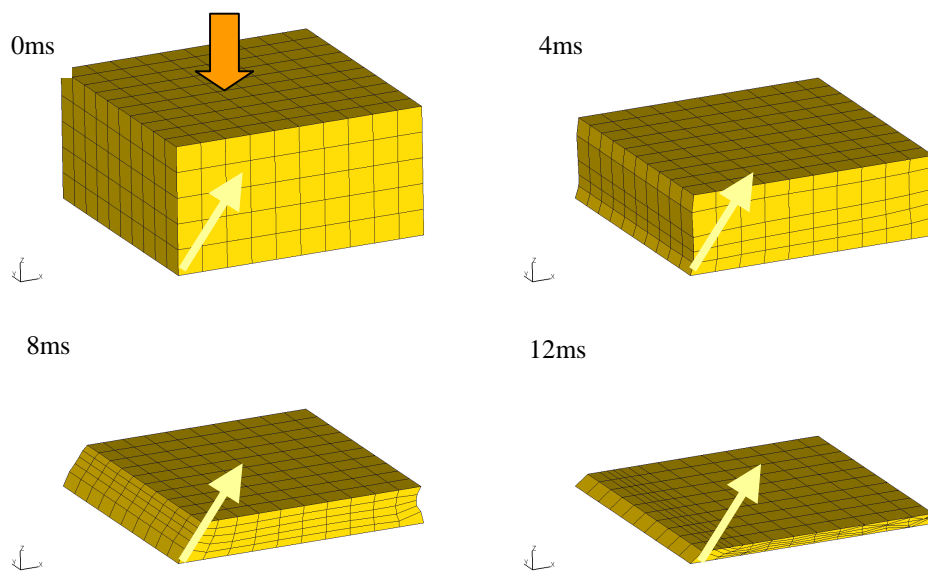


**Figure 6.** Simulation of *Strandfoam 2.5pcf* with 35° offset load (light arrow)

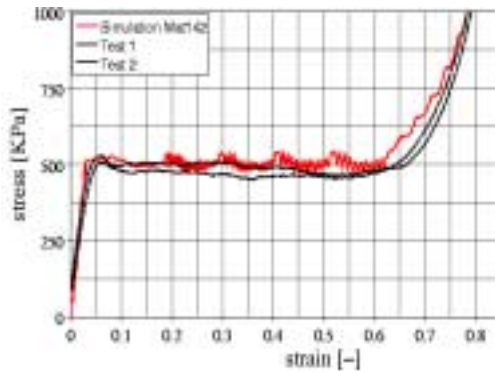
The forces measured under offset loading cannot be directly converted into stress/ strain curves that serve as input for the numerical model. There are a number of reasons for this:

- The shear deformation under off-axis loading means that the angle  $\vartheta$  between loading direction and longitudinal (extrusion) direction of the foam is not constant during the test.
- The friction effects in the test mean that we cannot reproduce the exact boundary conditions, the theoretical derivations in “*Material law MAT\_HONEYCOMB (Mat 26)*” are based on a free sliding boundary condition on both upper and lower surface.
- The state of stress and state of strain are not homogeneous in all samples tested under off-axis loading.

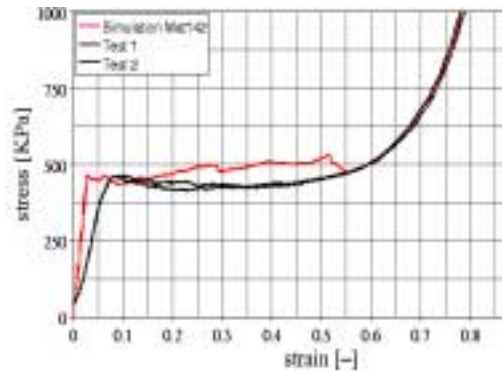
Consequently some trial-and-error might allow a better fit of the model to the measured results.

In the following pictures (figure 7) a global overview of simulation and direct comparison to testing is given.

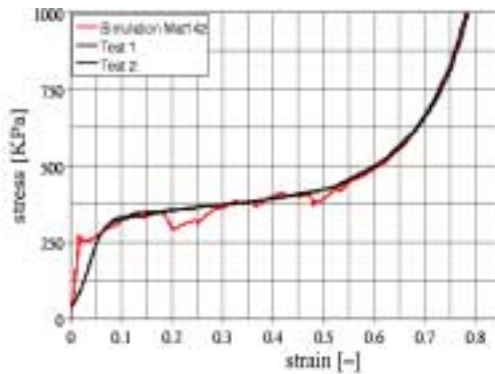
### Dynamic compression: 0°



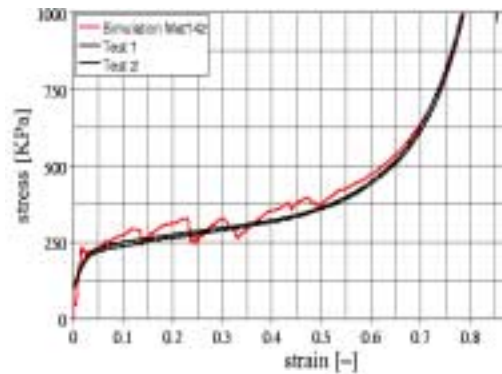
### Dynamic compression: 10°



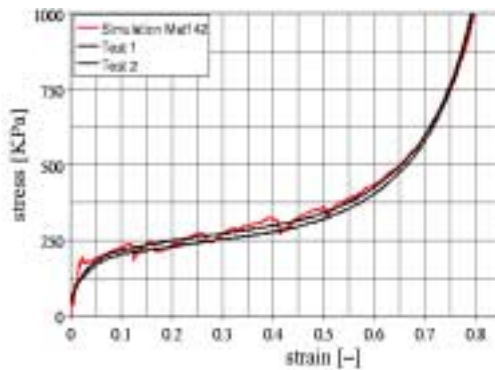
### Dynamic compression: 35°



### Dynamic compression: 45°



### Dynamic compression: 60°



### Dynamic compression: 90°

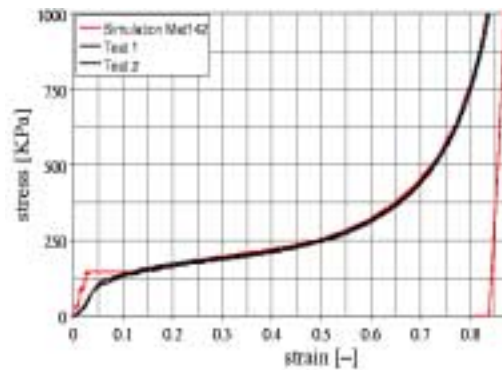
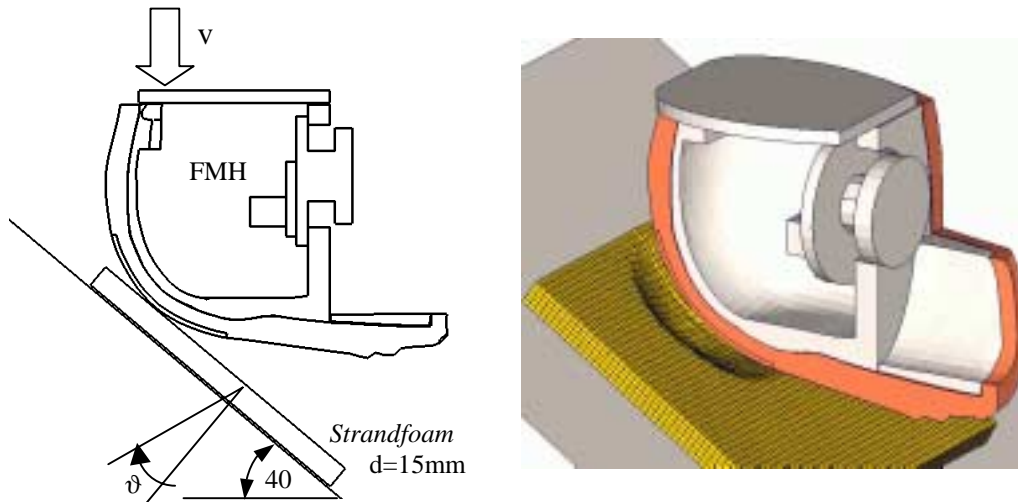


Figure 7. Overview of simulation (red line) in comparison to testing (dotted black line)

### Application to FMVSS201 head-impact

A typical application of the *Strandfoam* material is head-impact protection according to FMVSS201. It is felt that the angle between the impact direction and the extrusion direction of the foam will have an influence on measured headform accelerations. In order to illustrate this, an idealized setup was simulated where the FMVSS201 headform model impacts a rigid inclined plate. The plate is covered with a 15mm

thick block of *Strandfoam*, the extrusion direction of which is varied relative to the normal of the plate ( $0^\circ$ ,  $90^\circ$  and  $-30^\circ$ ). The simulation setup and a typical result are shown in figure 8.



**Figure 8.** left: FMHSS201 headform impacting a skewed plate with *Strandfoam* cover  
right: final deformed shape of the baseline ( $\vartheta = 0^\circ$ )

It should be emphasized that the only modification necessary in the dataset to examine different extrusion directions is the orientation vector in the material law definition. The simulation results in terms of head resultant acceleration time histories are shown in figure 9 for all three different extrusion directions.

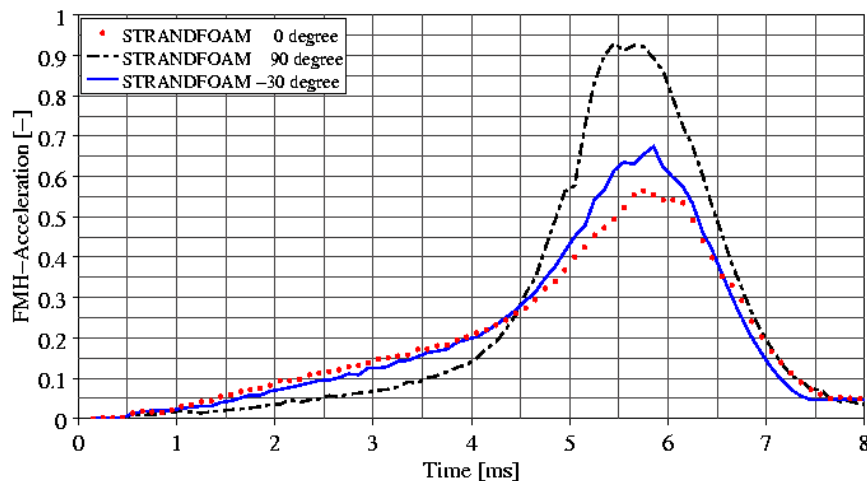


**Figure 9.** Head accelerations with three different extrusion directions in the *Strandfoam*

### **Application to honeycomb structures**

One of the main concerns in simulation work for automotive safety today is the modeling of aluminium honeycomb structures that constitute the energy-absorbing component of frontal-offset and side-impact test barriers.

To show the potential of the newly developed material model in this field we have simulated an impact test of the *Cellbond honeycomb* barrier against a concrete pole. The simulation was first performed using material law 26 in LS-DYNA and repeated while switching the material model to law 142.

The final deformed shapes for both simulations are shown below in figure 10.

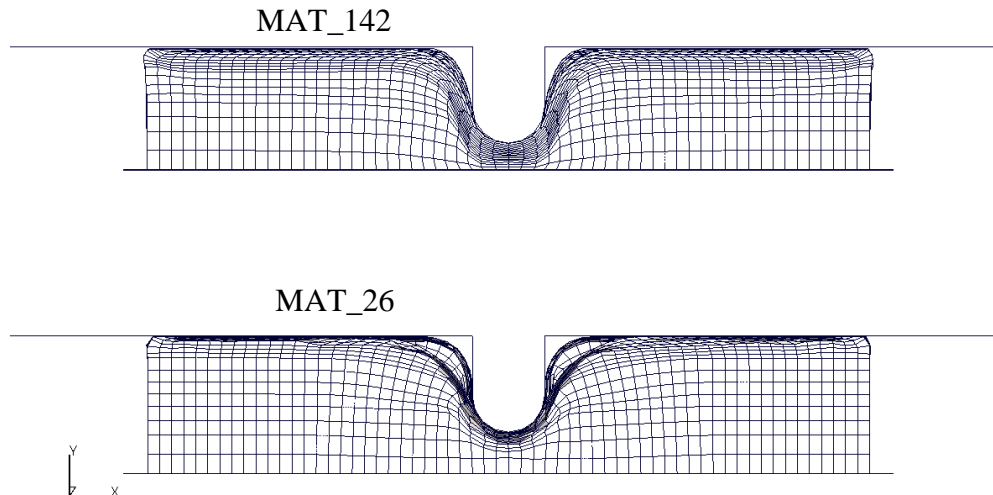


**Figure 10.** Final deformed shape of simulation using material laws 142 and 26

Although both input decks use the same stress-strain functions describing the honeycomb response in its strong and weak directions, the resulting strength under offset loading is a function of the material formulation as shown in figure 11. Here the off-axis strengths were determined as described in paragraph “Material law MAT\_HONEYCOMB (Mat 26)”.

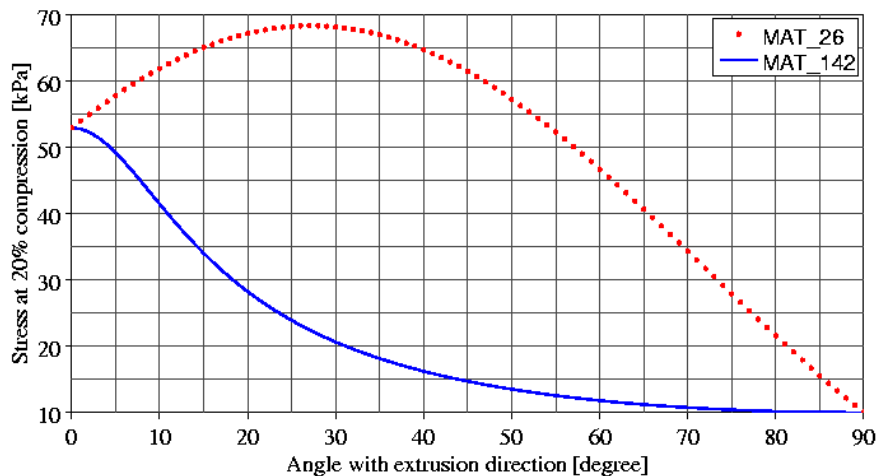


**Figure 11.** Off-axis strength for *Cellbond honeycomb* at 20% compression, theoretical values with Mat26 (red dotted line) and Mat142 (blue line)

The impact forces as a function of time resulting for both simulations are shown and compared to test values in figure 12. As could be expected, the simulation based on material law 26 shows a too high energy absorption prior to 60 milliseconds, and consequently no densification occurs in this model.



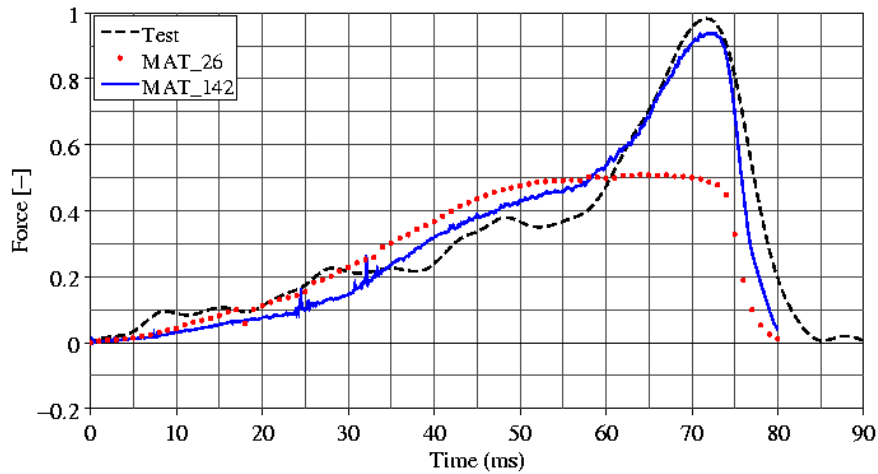


**Figure 12.** Overview of simulation using material law 26 (dotted red line) and material law 142 (blue line) in comparison to testing (dashed black line)

## SUMMARY OF CONCLUSIONS

A transversely anisotropic crushable material model for low-density foams was developed. The results in the simulation of *Strandfoam* allow the numerical simulation of the off-axis material response with good accuracy. Another possible application lies in the simulation of honeycomb for barriers used in frontal-offset and side-impact testing.

## REFERENCES

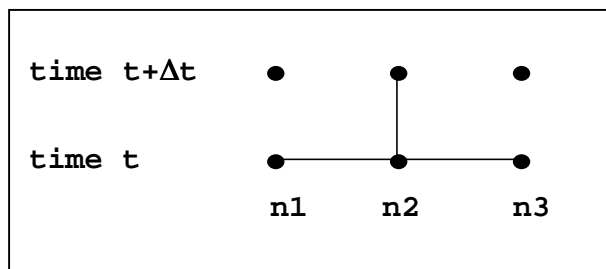
1. LS-DYNA, structured user's manual, version 950, LSTC

#### 4. The Next Step

This chapter builds on the simple example presented in the previous chapter. First, more detail is given about solving this problem using explicit analysis in section 4.1. Explicit analysis is well suited to dynamic simulations such as impact and crash analysis, but it can become prohibitively expensive to conduct long duration or static analyses. Static problems, such as sheet metal spring back after forming, are one application area for implicit analysis. Implicit analysis is presented in section 4.2. The difference between explicit and implicit is described. The problem is then presented as a heat transfer problem in section 4.3 and finally as a coupled thermal-stress problem in section 4.4.

##### 4.1 Explicit Analysis (problem ex01.k)

Explicit refers to the numerical method used to represent and solve the time derivatives in the momentum and energy equations. The following figure presents a graphical description of



explicit time integration. The displacement of node n2 at time level t+Δt is equal to known values of the displacement at nodes n1, n2, and n3 at time level t. A system of explicit algebraic equations are written for all the nodes in the mesh at time level t+Δt. Each equation is solved in-turn for the unknown node point displacements. Explicit methods are computational fast but are conditionally stable. The time step, Δt, must be less than a critical value or computational errors will grow resulting in a bad solution. The time step must be less than the length of time it takes a signal traveling at the speed of sound in the material to traverse the distance between the node points. The critical time step for this problem can be calculated by

$$\Delta t \leq \frac{\Delta x}{c} = \frac{\Delta x}{\sqrt{\frac{E}{\rho}}} = \frac{1.}{\sqrt{\frac{70. * 10^9}{2700.}}} = 1.96 * 10^{-4} \text{ sec}$$

To be safe, the default value used by LS-DYNA is 90% of this value or 1.77e-04 sec. Therefore, this problem requires 5,658 explicit time steps as compared with 10 implicit time steps (see section 4.2). Note that the time step and scale factor can be set using the keyword `*CONTROL_TIMESTEP`.

The input file for the 1-element aluminum cube example problem, presented in Chapter 3, is duplicated below. The keyword `*TITLE` has been added for problem identification.

### Example 4-1 Aluminum cube deformation, explicit method (file: ex01.k)

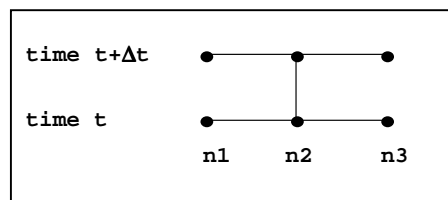
```

*KEYWORD
*TITLE
ex01.k - explicit analysis, problem 1
$
$----- define solution control and output parameters -----
$
*CONTROL_TERMINATION
1.
*DATABASE_BINARY_D3PLOT
.1
$
$----- define model geometry and material parameters -----
$
*PART
aluminum block
1
1
1
*SECTION_SOLID
1
1
*MAT_ELASTIC
1
2700. 70.e+09 .3
*NODE
1 0. 0. 0. 7 7
2 1. 0. 0. 5 0
3 1. 1. 0. 3 0
4 0. 1. 0. 6 0
5 0. 0. 0. 1. 4 0
6 1. 0. 0. 1. 2 0
7 1. 1. 1. 0 0
8 0. 1. 1. 1. 1 0
*ELEMENT_SOLID
1 1 1 2 3 4 5 6 7 8
$
$----- define boundary conditions and load curves -----
$
*LOAD_SEGMENT
1 1. 0. 5 6 7 8
*DEFINE_CURVE
1
0. 0.
1. 70.e+05
*END

```

### 4.2 Implicit Analysis (problem im01.k)

Implicit refers to the numerical method used to represent and solve the time derivatives in the momentum and energy equations. The following figure presents a graphical description of implicit time integration.



The displacement of node  $n_2$  at time level  $t+\Delta t$  is equal to known values of the displacement at nodes  $n_1$ ,  $n_2$ , and  $n_3$  at time level  $t$ , and also the unknown displacements of nodes  $n_1$  and  $n_3$  at time level  $t+\Delta t$ . This results in a system of simultaneous algebraic equations that are solved using matrix algebra (e.g., matrix inversion). The advantage of this approach is that it is unconditionally stable (i.e., there is no critical time step size). The disadvantage is the large numerical effort required to form, store, and invert the system of equations. Implicit simulations typically involve a relatively small number of computationally expensive time steps.

The keyword `*CONTROL_IMPLICIT_GENERAL` is used to activate the implicit method. The second entry on this card is the time step. For this example the time step is 0.1 sec. Therefore, a total of 10 implicit time steps will be taken to solve this problem. The results are identical to those obtained by the explicit method as shown in Sec 3.3.

For small problems, such as this 1 element example, most of the computer time is spent performing IO operations in reading the data and writing the output files. Very little CPU time is spent solving the problem. No conclusions should be made concerning the execution speed of explicit versus implicit methods on this problem.

**Example 4-2 Aluminum cube deformation, implicit method (file: im01.k)**

```

*KEYWORD
*TITLE
im01.k - implicit analysis - problem 1
$
$----- implicit solution keywords -----
$
*CONTROL_IMPLICIT_GENERAL 1 .1
$
$----- define solution control and output parameters -----
$
*CONTROL_TERMINATION
1.
*DATABASE_BINARY_D3PLOT
.1

```

This keyword turns on the implicit method

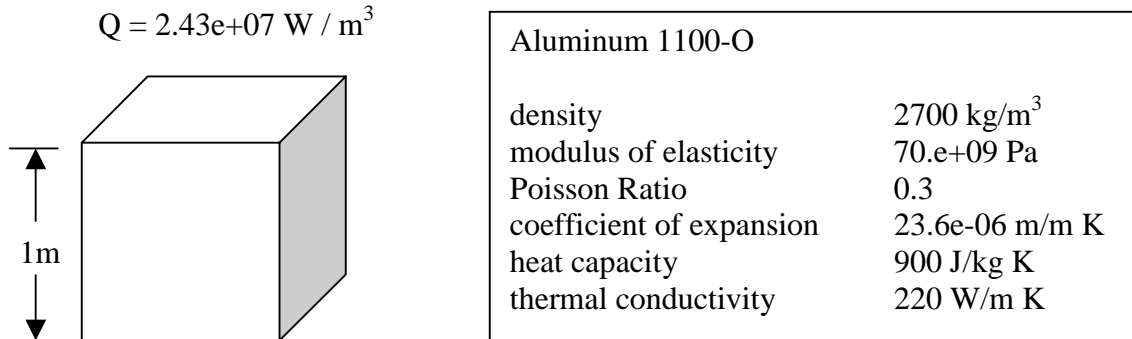
```

$
$----- define model geometry and material parameters -----
$
*PART
aluminum block
1 1 1
*SECTION_SOLID
1
*MAT_ELASTIC
1 2700. 70.e+09 .3
*NODE
1 0. 0. 0. 7 7
2 1. 0. 0. 5 0
3 1. 1. 0. 3 0
4 0. 1. 0. 6 0
5 0. 0. 1. 4 0
6 1. 0. 1. 2 0
7 1. 1. 1. 0 0
8 0. 1. 1. 1 0
*ELEMENT_SOLID
1 1 1 2 3 4 5 6 7 8
$
$----- define boundary conditions and load curves -----
$
*LOAD_SEGMENT
1 1. 0. 5 6 7 8
*DEFINE_CURVE
1
0. 0.
1. 70.e+05
*END

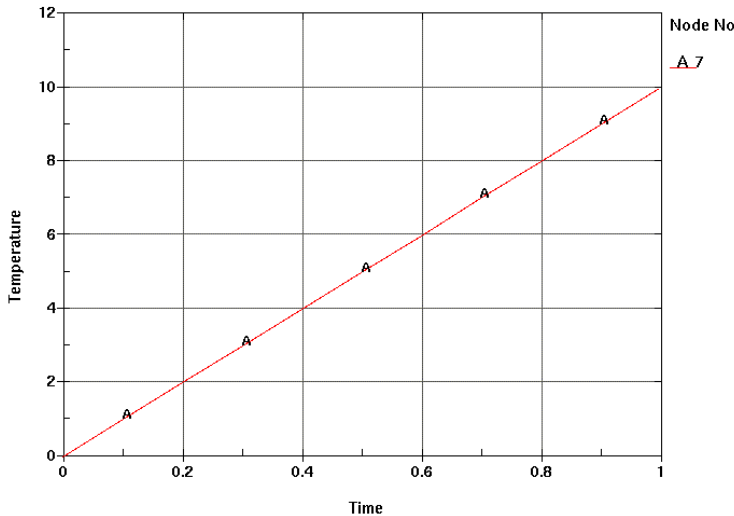
```

### 4.3 Heat Transfer Analysis (problem th01.k)

LS-DYNA can solve steady state and transient heat transfer problems. Steady state problems are solved in one step, while transient problems are solved using an implicit method. Our 1-element problem will now be re-defined as a transient heat transfer problem as shown below:



We will solve for the temperature response of the cube as the result of internal heat generation, Q. All the surfaces of the cube are perfectly insulated. Therefore, all the heat generation goes into increasing the internal energy of the cube. The temperature response of the cube calculated by LS-DYNA is shown in the figure below. The analytical solution is shown in the box.



$$T = \frac{Qt}{\rho V c_p}$$

$$T = \frac{(2.43e + 07)(t)}{(2700.)(1)(900.)}$$

$$T = 10t$$

The keyword input for this problem is shown below. Important things to note are:

- The default initial condition is T=0 for all nodes.
- The default thermal boundary condition is adiabatic (i.e. perfectly insulated). Therefore, no thermal boundary conditions need be specified for this problem.
- The \*CONTROL\_SOLUTION keyword is used to specify this problem as thermal only.
- The entry on the \*PART keyword points to the definition of thermal property data
- The entry on the \*PART keyword points to the definition of thermal property data.

**Example 4-3 Aluminum cube transient heat transfer analysis (file: th01.k)**

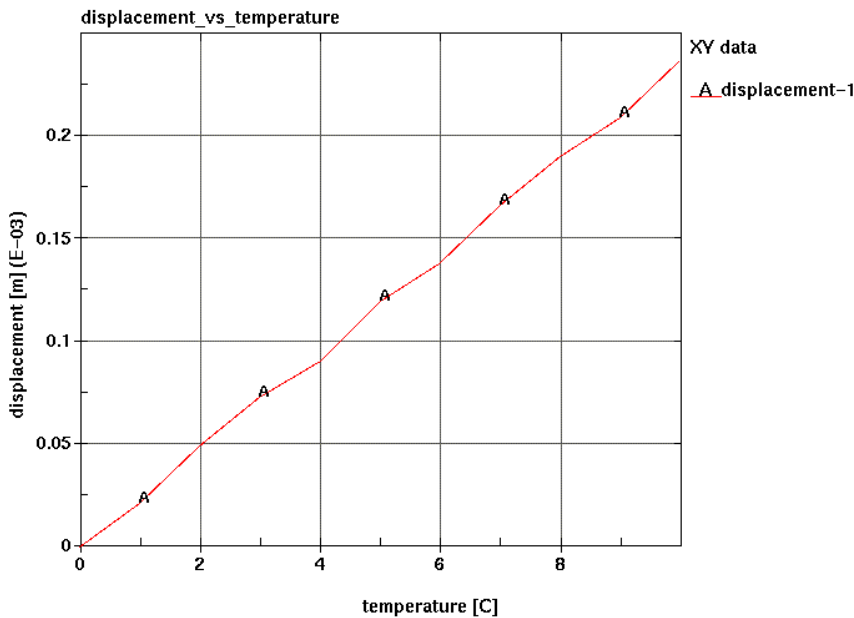
```

*KEYWORD
*TITLE
th01.k - heat transfer - problem 1
$
$----- thermal solution keywords -----
$
*CONTROL_SOLUTION 1
*CONTROL_THERMAL_SOLVER 1
*CONTROL_THERMAL_TIMESTEP 0 1. .1
*DATABASE_TPRINT .1
$
$----- define solution control and output parameters -----
$
*CONTROL_TERMINATION 1.
*DATABASE_BINARY_D3PLOT .1
$
$----- define model geometry and material parameters -----
$
*PART
aluminum block
1 1
*SECTION_SOLID 1
*MAT_THERMAL_ISOTROPIC 1 2700. 0 2.43e+07
904. 222.
*NODE
1 0. 0. 0. 7 7
2 1. 0. 0. 5 0
3 1. 1. 0. 3 0
4 0. 1. 0. 6 0
5 0. 0. 1. 4 0
6 1. 0. 1. 2 0
7 1. 1. 1. 0 0
8 0. 1. 1. 1 0
*ELEMENT_SOLID
1 1 1 2 3 4 5 6 7 8
*END

```

#### 4.4 Coupled thermal-stress analysis (problem cp01.k)

In this problem, the cube is allowed to expand due to the temperature increase from internal heat generation. Keywords from the mechanical problem defined in section 4.1 and the thermal problem defined in section 4.3 are combined to define this thermal-stress problem. The keyword \*MAT\_ELASTIC\_PLASTIC\_THERMAL is used to define a material with a thermal coefficient of expansion. For this problem,  $\alpha = 23.6 \cdot 10^{-6}$  m/m C. The aluminum blocks starts out at 0C (the default initial condition) and heats up 10C over the 1 second time interval (see section 1.3 above). The x displacement of node 7 versus temperature increase as calculated by LS-DYNA is shown in the figure below. The curve is not smooth due to numerical noise in the solution because we are only using 1 element. The analytical solution is shown in the box.



$$\begin{aligned} \Delta x &= \alpha \Delta T \\ &= (23.6e - 06)(10) \\ &= 23.6e - 05 \end{aligned}$$

The keyword input for this problem is shown below. Important things to note are:

- \*CONTROL\_SOLUTION is set to 2. This defines the problem as a coupled thermal stress analysis.
- Defining both mechanical and thermal properties.
- Using a mechanical constitutive model (\*MAT\_ELASTIC\_PLASTIC\_THERMAL) that allows entry of a thermal coefficient of expansion and mechanical properties that are a function of temperature.
- The mechanical and thermal time steps are independent. For this problem, we are using the default explicit mechanical time step calculated by the code and have specified a thermal time step of 0.1 sec. Therefore, many mechanical time steps will be taken for every thermal time step.



**Example 4-4 Aluminum cube coupled thermal-stress solution (file: cp01.k)**

```

*KEYWORD
*TITLE
cp01.k - coupled thermal stress analysis - problem 1
$
$----- define solution control and output parameters -----
$
*CONTROL_SOLUTION 2
*CONTROL_TERMINATION 1.
*DATABASE_BINARY_D3PLOT .1
$
$----- thermal solution keywords -----
$
*CONTROL_THERMAL_SOLVER 1
*CONTROL_THERMAL_TIMESTEP 0 1. .1
*DATABASE_TPRINT .1
$
$----- define model geometry and material parameters -----
$
*PART
aluminum block
1 1
*SECTION_SOLID 1
*MAT_ELASTIC_PLASTIC_THERMAL 1 2700.
0. 100.
70.e+09 70.e+09
.3 .3
23.6e-06 23.6e-06
*MAT_THERMAL_ISOTROPIC 1 2700.
904. 222.
0 2.44e+07
*NODE
1 0. 0. 0. 7 7
2 1. 0. 0. 5 0
3 1. 1. 0. 3 0
4 0. 1. 0. 6 0
5 0. 0. 1. 4 0
6 1. 0. 1. 2 0
7 1. 1. 1. 0 0
8 0. 1. 1. 1 0
*ELEMENT_SOLID 1 1 1 2 3 4 5 6 7 8
*END

```

**FEA Information News Previously Showcased  
Archived on the site on the News Page**

May 04	CEI	EnSight
	AMD	AMD Opteron
	Theme	Distributor in Korea
May 11	ANSYS	DesignSpace V. 6.1
	JRI	JMAG-Studio
	ANSYS – China	Distributor in China
May 25	LSTC	Conference
	MSC.Software	MSC.Linux
	Cril Technology	Distributor in France

**EVENTS – see events on [www.feainformation.com](http://www.feainformation.com) for details**

<b>2002</b>		
Sept 16 – 17	Sweden	Nordic LS-DYNA Users' Conference
Sept. 18 & 19	USA	LMS Conference for Physical and Virtual Prototyping
Sept. 19&20	Germany	DYNAMore – German LS-DYNA Forum
Oct. 03-04	Italy	Engin Soft Conference and User's Meeting
Oct. 08	UK	OASYS LS-DYNA Update Meeting
Oct. 09-11	Germany	CAD-FEM Users Meeting - Germany
Oct. 10-13	USA	10 <sup>th</sup> Foresight Institute Conference on Molecular Nanotechnology
Oct. 24 – 25	Japan	Japanese LS-DYNA & JMAG Users Conference
Oct. 28	Korea	Korean LS-DYNA Users Conference
Nov. 28 & 29	Germany	LMS Conference for Physical and Virtual Prototyping
Dec 18 – 21	India	HiPC 2002
<b>2003</b>		
May 19-21	USA	BETECH2003
May 22-23	Germany	4 <sup>th</sup> European LS-DYNA Conference
June 17-20	USA	The Second M.I.T Conference on Computational Fluid and Solid Mechanics

## Visteon Uses Advanced Visualization to Give Passengers a Safe, Smooth Ride

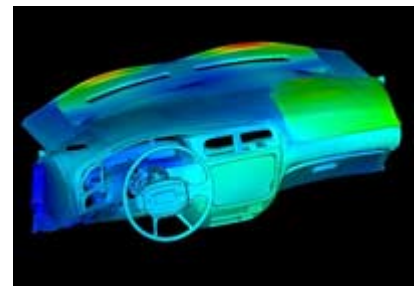
Reprinted from  
website: <http://www.ensight.com/news/visteon.html>

DEARBORN, Mich., January 11, 2002 - When it comes to buying a car, consumers might desire speed and style, but ultimately rider comfort and safety are key factors in purchase decisions. Visteon Corp. (NYSE: VC), a leading supplier of integrated automotive technology systems, helps 19 of the largest vehicle manufacturers in the world ensure a smooth, safe ride for their customers.

### If You Can't Stand the Heat, Get Out of the Car

Visteon uses advanced visualization software to analyze how automotive interior elements react under specific conditions. Researchers completed a simulation showing thermal stress and heat expansion on the dashboard of a Ford Taurus left in the Arizona summer sun. The engineering team used **EnSight** software from CEI (Apex, N.C.) to visualize **MSC.Nastran** data on the deformation contours created when the closed automobile reached temperatures in excess of 235 degrees Fahrenheit.

This and other complex automotive applications typically generate models with between 500,000 and 1 million degrees of freedom (DOF). Working with such large models makes clear visualizations imperative for engineers, according to Kumar Kulkarni, a technical specialist at Visteon. "We need a distinct visual to help us examine and understand these big datasets. Great 3D effects and keyframe animation sequences make the results easier to interpret."



### Communication Through 3D Animation

Visteon engineers also use **EnSight** for automotive interior and safety simulations. Analyzing specific design factors, such as how a steering column vibrates, helps manufacturers reduce noise, vibration and harshness inside the vehicle interior. In addition to ensuring a smooth, quiet ride, gathering performance data about a vehicle's design can help keep passengers safe. Visteon researchers view **LS-Dyna** crash simulation results in **EnSight** to analyze how occupant energy is dissipated when test dummies impact a vehicle's instrument panel.

Once an engineering solution is reached, visualization still has an important role according to Kulkarni. "Using the visualization as a communication tool is as important as the analysis itself," he says. "Visualization software allows us to share our findings with management, customers and other engineers."

Publicly launched in 1997 at the Frankfurt Motor Show, Visteon Corp. is one of the largest automotive suppliers in the world. The company has nearly 80,000 employees in 25 countries. Visteon's global sales revenues in 2000 reached \$19.5 billion. The company has over 80 years

experience in accomplished integration systems. For company and product information, visit [www.visteon.com](http://www.visteon.com).

CEI provides complete solutions for analyzing, visualizing and communicating engineering and scientific computational results. The CEI product line ranges from EnSight and EnSight Gold visualization software to EnLiten, EnVideo and EnVe, free software packages that enable EnSight models and animations to be edited and shared over the Internet. CEI also provides consulting services to engineers and scientists from organizations that use computational methods for research, product design or product refinement.

### FEA Information Inc. Commercial & Educational Participants

Headquarters	Company	
Australia	Leading Engineering Analysis Providers	<a href="http://www.leapaust.com.au">www.leapaust.com.au</a>
Belgium	LMS, International	<a href="http://www.lmsintl.com">www.lmsintl.com</a>
Canada	Metal Forming Analysis Corp.	<a href="http://www.mfac.com">www.mfac.com</a>
China	ANSYS Beijing	<a href="http://www.ansys.com">www.ansys.com</a> (link on international)
France	Dynalis – Cril Technology Simulation	<a href="http://www.criltechnology.com">www.criltechnology.com</a>
Germany	DYNAMore	<a href="http://www.dynamore.de">www.dynamore.de</a>
Germany	CAD-FEM	<a href="http://www.cadfem.de">www.cadfem.de</a>
India	GissEta	<a href="http://www.gisseta.com">www.gisseta.com</a>
Italy	Altair Engineering srl	<a href="http://www.altairtorino.it">www.altairtorino.it</a>
Japan	The Japan Research Institute, Ltd	<a href="http://www.jri.co.jp">www.jri.co.jp</a>
Japan	Fujitsu Ltd.	<a href="http://www.fujitsu.com">www.fujitsu.com</a>
Korea	THEME Engineering	<a href="http://www.lsdyna.co.kr">www.lsdyna.co.kr</a>
Korea	Korean Simulation Technologies	<a href="http://www.kostech.co.kr">www.kostech.co.kr</a>
Russia	State Unitary Enterprise - STRELA	<a href="http://www.ls-dynarussia.com">www.ls-dynarussia.com</a>
Sweden	Engineering Research AB	<a href="http://www.erab.se">www.erab.se</a>
Taiwan	Flotrend Corporation	<a href="http://www.flotrend.com">www.flotrend.com</a>
UK	OASYS, Ltd	<a href="http://www.arup.com/dyna">www.arup.com/dyna</a>
USA	Livermore Software Technology	<a href="http://www.lstc.com">www.lstc.com</a>
USA	Engineering Technology Associates	<a href="http://www.eta.com">www.eta.com</a>
USA	ANSYS, Inc	<a href="http://www.ansys.com">www.ansys.com</a>
USA	Hewlett Packard	<a href="http://www.hp.com">www.hp.com</a>
USA	SGI	<a href="http://www.sgi.com">www.sgi.com</a>
USA	MSC.Software	<a href="http://www.mssoftware.com">www.mssoftware.com</a>
USA	EASi Engineering	<a href="http://www.easiusa.com">www.easiusa.com</a>
USA	DYNAMAX	<a href="http://www.dynamax-inc.com">www.dynamax-inc.com</a>
USA	CEI	<a href="http://www.ceintl.com">www.ceintl.com</a>
USA	AMD	<a href="http://www.amd.com">www.amd.com</a>
USA	Dr. T. Belytschko	Northwestern University
USA	Dr. D. Benson	Univ. California – San Diego
USA	Dr. Bhavin V. Mehta	Ohio University
USA	Dr. Taylan Altan	The Ohio State U – ERC/NSM
USA	Prof. Ala Tabiei	University of Cincinnati
Russia	Dr. Alexey I. Borokov	St. Petersburg State Tech. University
Italy	Prof. Genarro Monacelli	Prode – Elasis & Univ. of Napoli, Federico II

## FIRST ANNOUNCEMENT AND CALL FOR PAPERS

4<sup>th</sup> EUROPEAN LS-DYNA CONFERENCE  
22<sup>nd</sup> - 23<sup>rd</sup> OF MAY 2003, ULM, GERMANY

The 4<sup>th</sup> European LS-DYNA Users' Conference will be held in Germany in May 2003. This conference will provide an ideal forum for LS-DYNA users from all over the world to share and discuss their experiences, to obtain information on up-coming features of LS-DYNA and to learn more about new application areas.

The conference will be accompanied by an exhibition featuring the latest software and hardware developments related to LS-DYNA.

We expect attendees and presenters from all over the world highlighting the numerous different application areas of LS-DYNA. In addition, you will also have the chance to follow lectures from developers from LSTC on the newest features of LS-DYNA. Dr. John Hallquist will be a keynote speaker.

The conference will take place in Ulm, the birthplace of Albert Einstein. The hotel is located right next to the famous river Danube. From the hotel you will have a marvellous view of the old town of Ulm with the historic cathedral in the centre. You have the opportunity to climb the highest cathedral tower in the world, its construction started in 1377.

The European LS-DYNA conference is organized by a group of European LS-DYNA distributors and takes place every other year. The 4<sup>th</sup> conference will be organized in 2003 under the leadership of DYNAmore with assistance from:



LS-DYNA distributors in Germany - DYNAmore, United Kingdom - ARUP, France - CRIL TECHNOLOGY Simulation, the Nordic Countries - ERAB, and Russia - STRELA.

Questions regarding your paper please feel free to contact:

Dr. Heiner Müllerschön at DYNAmore GmbH  
Phone: +49 (0)7 11 - 45 96 00 - 0  
E-mail: hm@dynamore.de

Additional information on the organizers is available at:

[www.dynamore.de](http://www.dynamore.de)  
[www.arup.com/dyna](http://www.arup.com/dyna)  
[www.erab.se](http://www.erab.se)  
[www.criltechnology.com](http://www.criltechnology.com)  
[www.ls-dynarussia.com](http://www.ls-dynarussia.com)